A cryogenic cooling system for restoring IR science on the Hubble Space Telescope

Nicholas M. Jedrich[a], Teri H. Gregory[a], Darrell Zimbelman[b], Edward S. Cheng[b], Larry D. Petro[c], Christine E. Cottingham[d], Matt T. Buchko[e], Marc L. Kaylor[e], Francis X. Dolan[f]

[a]Jackson & Tull, 7375 Executive Place, Suite 200, Seabrook, MD 20706; [b]NASA Goddard Space Flight Center, Greenbelt, MD 20771; [c]Space Telescope Science Institute 3700 San Martin Drive Baltimore, MD 21218; [d]Lockheed Martin Technical Operations, 7474 Greenway Center Drive, Suite 200, Greenbelt, MD 20770; [e]Swales Aerospace Incorporated, 5050 Powder Mill Rd, Beltsville, MD 20705; [f]Creare Incorporated, Etna Road, Hanover, NH 03755

ABSTRACT

This paper presents a description of the Hubble Space Telescope (HST) Near Infrared Camera and Multi Object Spectrometer (NICMOS) Cooling System (NCS), the evolution of the cutting edge technology involved, a comparison of predicted versus on-orbit thermal performance, as well as possible future space applications. The NCS hardware consists of the NICMOS Cryogenic Cooler (NCC), an Electronics Support Module (ESM), a Capillary Pumped Loop (CPL)/Radiator assembly, and associated interface harnessing. The NCC is a state-of-the-art reverse Turbo-Brayton cycle mechanical cooler employing micro turbo machinery, driven by advanced power conversion electronics, operating at speeds up to 450,000 revolutions per minute to remove heat from the NICMOS instrument. The ESM provides command, control, and power distribution to the NCS, as well as providing the primary interface to the existing HST electronics. A two-phase CPL system removes heat from the NCC and transfers it to the radiator mounted externally on the HST aft shroud. The system was installed during Servicing Mission 3B via extravehicular activities in March 2002. The NCS revived the NICMOS instrument, which experienced a reduced operational lifetime due to an internal thermal short in its dewar structure, and restored HST scientific infrared capability to operational status.

Keywords: cryogenics, instrument cooling systems, HST, capillary pumped loop, NICMOS

1. MOTIVATION

1.1 Near Infrared Camera and Multi Object Spectrometer instrument

The Near Infrared Camera and Multi-Object Spectrometer (NICMOS) is a second generation Hubble Space Telescope (HST) scientific instrument installed during Servicing Mission 2 in February of 1997. The instrument is designed to provide infrared imaging and limited spectroscopic observations of targets between 1.0 and 2.5 microns using three cameras housed in a cold well inside a cryogenic dewar. The NICMOS instrument allows the investigation of two unique scientific areas, the distant universe by observing light emission in the infrared and the dust-enshrouded universe due to the longer near-infrared wavelengths not being as obscured by interstellar dust as visible wavelengths. NICMOS is the only infrared instrument currently installed on HST.

1.2 NICMOS thermal short

The hybrid solid nitrogen/aluminum foam dewar, surrounding the NICMOS cold optics bench, was designed to maintain a nominal detector environment of 58K with a stability of ±2K. The design includes three thermal shields that encase the dewar to provide cooling: the Vapor Cooled Shield (VCS), the Thermo-Electric Cooled Inner (TECI) Shield, and the Thermo-Electric Cooled Outer (TECO) Shield. The initial construction of the NICMOS dewar provided an ambient gap of 5 $\pm$ 1.2 mm between the cryogen tank forward closure cover and the VCS at three baffles. Following launch and instrument installation, an additional heat load of 422 mw was discovered causing an increased rate of cryogen sublimation reducing the dewar lifetime from an anticipated 60 months to an actual operation of 22 months. In addition, the higher heat load increased the internal detector temperature from 58K (the design set point) to 60K. Post launch

investigation determined that the VCS gap closed and created the heat load. The gap closure was attributed to an unexpected racheting effect coupled with high thermal expansion of the solid nitrogen within the NICMOS dewar during warm-up and subsequent cool-down cycles performed during ground handling.[1]

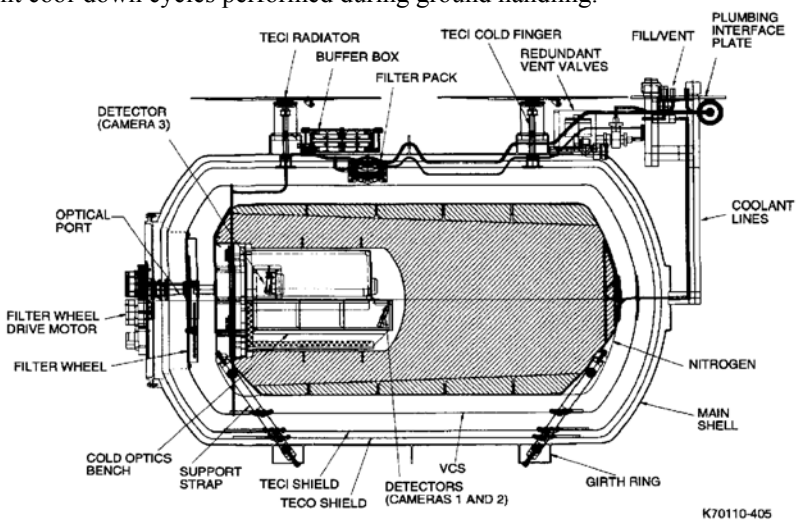

Figure 1 – NICMOS Dewar

1.3 NICMOS Cooling System solution

The depletion of the NICMOS dewar, coupled with the desire for IR science on HST through Servicing Mission 4, prompted the HST Project to investigate a long term hardware solution to restore NICMOS scientific operations.[2] The decision to develop the NICMOS Cooling System (NCS) required several non-standard HST interfaces including access to a mechanical coupling between the NCS and the NICMOS instrument. Fortunately, the NICMOS design provides a simple, male-to-female bayonet interface located on an external plumbing interface plate, which form a coolant loop used to circulate gaseous helium to convert the liquid nitrogen to a solid state during ground processing. This particular interface, shown in Figure 2, is accessible to astronauts during an Extra-Vehicular Activity (EVA) and would be used as a viable interface to begin development of a cryogenic cooling system to revive the NICMOS instrument

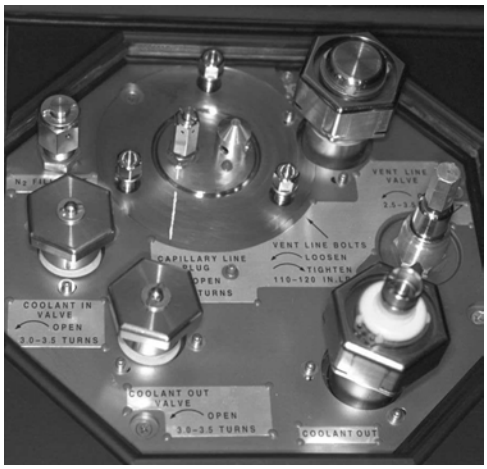

Figure 2 – Plumbing Interface Plate

With the interface to the instrument defined, additional requirements focusing on thermal performance and dynamic disturbance impacts to vehicle pointing performance were developed. The cooling system hardware was required to remove heat from the NICMOS, via the interface coolant loop, to provide a temperature of $\leq$75K at the detectors where effective imaging can occur by achieving a balance between quantum efficiency and the dark current count. This

requirement was set at 7 W and included system generated parasitic heat loads. A thermal stability of ±0.5K was also specified to minimize the need for repeated camera calibrations. For vehicle pointing performance, a derived requirement of 1 milli-arc second (mas) above the current HST pointing performance of 3 mas was selected for the cooling system.[3] The system also had to satisfy all existing HST mechanical and electrical interface requirements. The NCS was developed around these core requirements.

1.4 NICMOS cryostat concerns

One of the major technical concerns during the NCS design phase was the state of the NICMOS instrument. The shortened lifetime caused by an unexpected thermal short inside the cryostat called into question the mechanical state of the cryostat after warming up and during the initial cooldown with the NCS. In light of these concerns, the Project launched a major effort to monitor the details of the warmup, including temperatures and detector performance (where possible, during the initial part of the warmup). Detailed mechanical models including plastic deformation elements were built to verify the integrity of the cryostat and its continued thermal performance. All these models predicted that the cryostat would perform with the NCS as well as it had with the solid cryogen, and that the thermal short would remain roughly constant with the introduction of the NCS.

An additional concern was the venting of the getter gas in the cryostat vacuum jacket. Several charcoal getters are attached to the outside of the solid cryogen containment vessel (inside the vacuum jacket) to ensure vacuum integrity. When the cryostat warms up, the integrated gas is released into the jacket. If sufficient gas is released, it may become very difficult or impossible to achieve the desired detector temperatures. The gas release during warmup is reflected in the cryostat temperature curve were these characteristics were modeled in detail and coupled with the NCS operating model to predict on-orbit performance and margin. These models all predicted a modest positive margin for cooldown assuming worst-case conditions.

2. HARDWARE

The NCS hardware consists of the NICMOS Cryogenic Cooler (NCC), an Electronics Support Module (ESM), a Capillary Pumped Loop (CPL)/Radiator assembly, and associated interface harnessing. Figure 3 presents a schematic diagram of the NCS showing the major components and subsystems.

2.1 NCC

The NCC is a mechanical refrigerator employing high-speed, centrifugal turbomachines to cool and circulate gas through the coolant loop in the NICMOS cryostat. All the components, including the power conversion electronics (PCE), are contained in an aluminum housing attached to an aluminum honeycomb bridgeplate. Latches are utilized to secure the NCC to scientific instrument guiderail stand-offs and an EVA handhold in Bay 4 of the HST aft shroud.

In the cryocooler loop, neon gas is raised to a pressure ratio of about 1.6 by a centrifugal compressor operating at rotational speeds up to about 7300 rev/s. The gas flows from the aftercooler through an all-metal recuperator and then to the turboalternator where it expands through the turbine rotor and is cooled to produce refrigeration. The gas leaving the turbine flows through a cold load interface heat exchanger (CLI) and then through the low-pressure side of the recuperator back to the compressor inlet. Neon gas is pumped by a centrifugal circulator through the CLI to the NICMOS cooling coil in the circulator loop. This secondary loop was connected to the NICMOS cryostat during the servicing mission via flexible tubing and bayonet fittings to the interface shown in Figure 2. Heat from the instruments and structure is removed at the coil to maintain the required detector temperature. Heat is transferred to the cryocooler in the CLI with additional heat picked up in the circulating loop gas by conduction and radiation into the tubing and structure supporting the cold end components. The total heat load transferred across the CLI to the cryocooler is about 7 watts.

During operation, a three-phase motor drives the centrifugal compressor to provide overall cooling. Three-phase power for the motor is provided from an inverter in the PCE that converts unregulated spacecraft 28V DC to AC voltage and current at the desired frequency. The compressor speed (motor frequency) is changed in response to varying heat loads and rejection temperatures to maintain a constant temperature, within the stability requirements of ±0.5K at the detectors. A three-phase inverter in the PCE supplies less than 1 W of power to drive the circulator at a fixed speed of

1200 rev/s. This provides the required flow rate of neon through the cooling coil. The PCE also contains a set of load resistors connected to the turboalternator output to dissipate anywhere from 10 to 20 W of power in order to control the turbine shaft speed from 3000 rev/s to about 4500 rev/s. The heat from the cryocooler, the PCE electronics and the turboalternator load resistors is conducted through the heat rejection interface (HRI) to the capillary pump loop (CPL) evaporator where it is transported in the two-phase ammonia fluid loop to the spacecraft radiator.

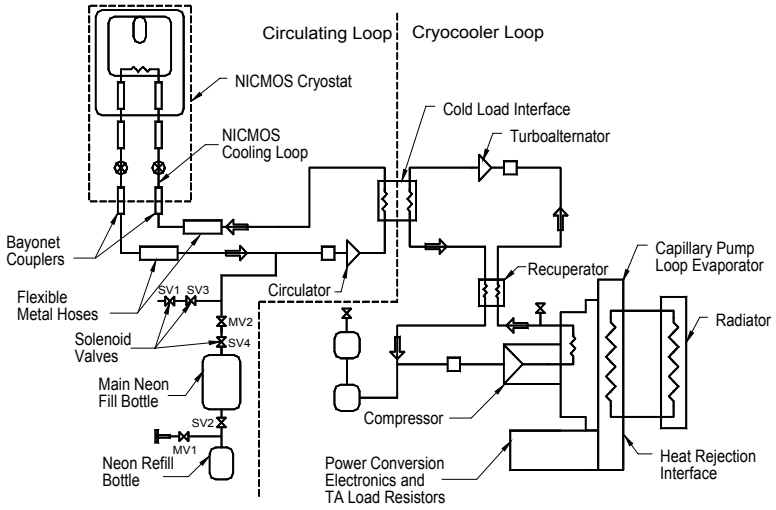

Figure 3 – NCS Block Diagram

2.2 CPL/radiator

The CPL evaporator pump is similar to the pump design first used on the CAPL-2 flight experiment and the Terra (EOS-AM) spacecraft. The CPL liquid and vapor transport lines are part rigid tubes and part metal bellows flexible hoses. The rigid tube length is approximately 2 meters (m), while the flexible hoses are in two sections with a total length of 3 m. The flexible hoses were required to aid the EVA crew in installing the system on HST. The radiator is mounted on the exterior of the aft shroud, via latches that attach to EVA handrails, in order to radiate the heat from the NCC to the space environment. A sock containing the long flexible CPL line sections and electrical harness, allows the EVA crew members to fed the lines through the cryovent port near NICMOS. A ninety-degree elbow in the conduit allows it to be locked into place at the cryovent providing structural rigidity and a light tight seal. The CPL wedge-shaped evaporator pump attached at the end of the flex hose installs onto a saddle mounted to the NCC housing opposite the NCC compressor. An embedded graphite thermal interface material (QPAD-3) is used to thermally couple the CPL evaporator and the saddle. A spring-loaded CPL Saddle cover provides the required contact pressure between the evaporator and saddle walls to maximize thermal conduction.

2.2.1 Radiator design

The NCS radiator design, presented in Figure 4, was driven by two factors: thermal efficiency and structural rigidity. Thermal analysis showed that a radiator efficiency of greater than 92% was required to remove the large NCC heat load (~450 W). The maximum allowable radiator size was determined to be 3.8 m in length and 1.2 m in width. However, all of this area is not available for heat rejection as 0.3 m^2 of the radiator is dedicated to subcooling. There are also two cutouts in the radiator perimeter to allow clearance for EVA accessible foot restraint sockets on the aft shroud of the telescope. The remaining area of approximately 2.7 m^2 contains an embedded header/spreader heat pipe network to isothermally dissipate the cryocooler heat load. The carrier and radiator attachment hardware used to ferry the NCS into orbit required the radiator panel to be stiff and strong. The core of the panel is 5 cm 4.4 PCF aluminum honeycomb the 0.13 cm 2024 aluminum facesheets. The radiator panel contains 16 spreader heat pipes and two header Heat Pipe Heat Exchangers (HPHX). The header heat pipes have integral HPHX's and are manufactured from a hexagonal cross-sectional axial groove heat pipe extrusion. The extrusion and helical fin HPHX design is identical to the heat exchanger

used in the Terra CPL systems. The HPHX's are plumbed in parallel and provide a highly efficient condenser for the NCS CPL.

2.2.2 Evaporator pump design

The CPL evaporator takes its design and fabrication heritage from the Swales TAG-54 aluminum Type 6063 evaporator pump. This baseline evaporator design has been used most recently on the CAPL-2/CAPL-3 flight experiments and the Terra satellite. The CPL pump is plumbed as a 3-port "Starter Pump" configuration. The pump has an internal bayonet attached to the reservoir supply line. The evaporator pump interfaces with the flexible stainless steel liquid return line via a stainless steel/aluminum bi-metallic fitting. The external configuration of evaporator was produced with a heavier wall thickness to facilitate the machining of the pump with a 3° wedge taper. The tapered wall provides very high compressive loads on the QPAD-3 material with relatively low torque loads on the saddle cover bolts.

2.2.3 Transport lines

The liquid and vapor transport lines connecting the evaporator pump and the radiator are comprised of smooth walled tubing and stainless steel flexible lines. The flexible hoses were used to facilitate the articulation of the CPL from the stowed to the installed position. The corrugated nature of the flex hoses increases the pressure drop in the CPL, specifically in the vapor transport lines, thereby reducing the total transport capability of the CPL. The additional pressure drop was taken into account in requiring liquid and vapor line flexible hoses with a nominal 0.98 cm inner diameter (ID). A section of the transport lines that spans across the aft shroud bulkhead is contained in the conduit. The conduit is a hollow 10 cm x 10 cm aluminum box that serves to contain and manage the electrical harness as well as CPL lines for EVA operations. The evaporator end of the conduit has a ring-collar designed to mate and hard-dock with the aft bulkhead cyrovent to allow the CPL evaporator and flex lines to enter the aft shroud and make a light tight seal. The transport lines within the conduit section are fabricated of smooth walled stainless steel tubing. The liquid line is 0.8 cm outer diameter (OD) with a 0.07 cm wall thickness and the vapor transport line is 0.9 cm OD with a 0.07 cm wall thickness.

A highly innovative design change for this CPL application was the incorporation of coaxial reservoir and liquid return lines. The CPL reservoir supply line runs coaxially within the liquid return line from the exit of the radiator to the inlet of the evaporator pump. The reservoir supply line is a 0.27 cm OD x 0.22 cm ID Teflon tube. During normal CPL operations the liquid in the reservoir line is essentially static, and the CPL operating temperature will typically be colder than the HST aft shroud environment. The coaxial configuration ensures that the reservoir line remains subcooled by the liquid flowing in the liquid return line, preventing vapor bubble formation in the reservoir line from parasitic heat leaks.

2.2.4 Reservoir design

The reservoir is used to manage the fluid inventory needs of the CPL and control the operating temperature of the system. The reservoir is cold biased to maintain positive control and is mounted on the radiator. To minimize the size and volume of the reservoir, it was determined that the CPL system would be launched charged, meaning that it would not be necessary to open any valves on orbit to fill the CPL with ammonia working fluid. The reservoir was sized to be 15% full during the minimum cold case and 80% full during the maximum hot case. The reservoir is fabricated of a 10.2 cm OD aluminum 6061 shell. The length of the reservoir assembly is 0.3 meters. The total volumetric displacement capacity is 60 cubic inches. An internal ultra high molecular weight polyethylene wick structure is used for internal fluid management. The reservoir temperature is controlled by a 15 W heater connected in a feedback control loop managed by the ESM microprocessor, and by cold biasing the reservoir via direct radiation to the environment. To increase the temperature of the reservoir rapidly if needed, an additional 50 W boost heater was installed. This heater is operated by ground command only. An MLI blanket incorporating a Kevlar layer for micrometeorite protection allows the reservoir to cool effectively, while minimizing the required controller heater power needed for steady state operation.

2.2.5 CPL temperature control

The cryocooler efficiency and power consumption is directly related to the temperature of the NCC compressor HRI, i.e. the CPL saddle. The Terra CPL systems operate at a fixed temperature, and the CAPL flight experiments were under continuous ground control. In order to take advantage of cold orbits, while protecting against hot orbits and possible CPL deprime, the NCS CPL operating temperature is variable and controlled autonomously by software in the ESM

8051 computer. A unique control algorithm was developed for the code that compares certain temperatures of CPL components and calculates the lowest operating temperature that can be obtained without exceeding the heat rejection capacity of the radiator, a situation that would cause the CPL to deprime. This code updates the reservoir control set point every half-second, works exceedingly well, requires no continuous ground support, and can be modified if the radiator coating optical properties deteriorate with age.

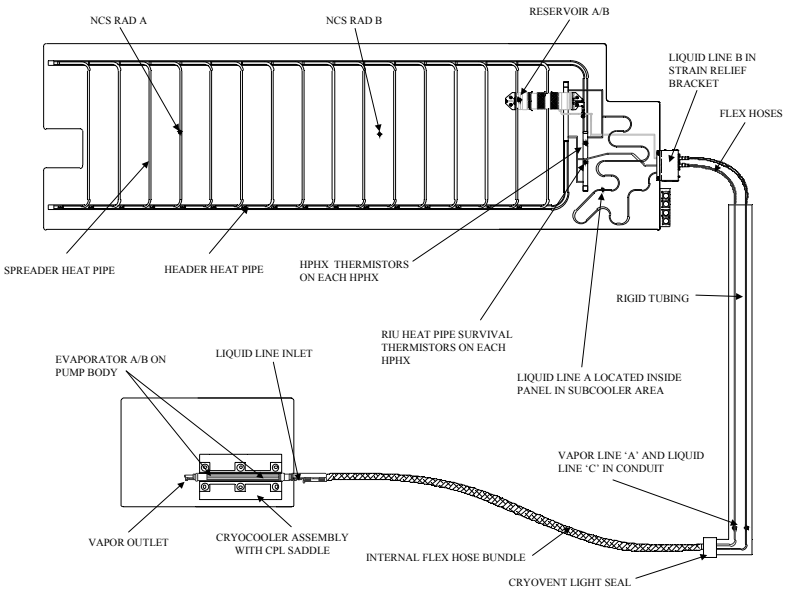

Figure 4 – CPL/Radiator Schematic

2.3 ESM and electrical interfaces

The ESM electronics provide command, control, and power distribution for the NCS. Two 8051 microprocessors provide redundant command and control of both the CPL/radiator and the NCC, while a single Power Switching and Distribution Unit (PSDU) distributes power. The ESM interface to the CPL/Radiator is through electrical harnesses run in parallel with the CPL ammonia lines from the radiator. The ESM interface to the NCC is through the Cross Aft Shroud Harness (CASH). The CASH carries both data and power from the ESM to the NCC. The interface to the HST command and data handling system is by two Remote Interface Units, one for each 8051 that interface through a Y-harness installed in the COSTAR data and power path. System power can be switched from either the Y-harness COSTAR source or the J600 source on HST.

3. TEST

The NCS test program consisted of a variety of tests, environmental and performance, to verify system requirements prior to launch and installation. Two critical thermal vacuum tests were performed on the NCS flight hardware in its final form to verifying the core thermal requirements, an NCC parasitic test and a NCS full-up system level thermal vacuum acceptance test.

3.1 NCC parasitic test results

During testing of the NCC it was important to quantify parasitic heat loads in the heat transport circulator loop since this governs the minimum temperature that can be achieved at the NICMOS detectors. The determination of parasitics was aided by the installation of a well-instrumented section of tubing, referred to as a shunt that connected the inlet and outlet heat transport lines of the NCC. This shunt and its instrumentation were thermally isolated from the NCC environment

so as not to introduce any additional parasitics. Using this shunt, the mass flow rate of the neon cooling gas and the distribution of parasitics throughout the heat transport loop of the NCC was able to be determined. The value of the method developed is that it provided a means to reliably quantify the cooling capability of the two-loop NCC and it provided a means to quantitatively evaluate modifications to the NCC to lower parasitics and therefore lower NICMOS detector temperature for better detector performance. [6]

Results of the testing and analysis predicted the parasitics in Table A.

Location	Parasitic (watts)	Uncertainty (watts)	See Note	Means of Determining
NICMOS Inlet Rigid Tubes	0.08	0.05	1	Test
Reinforcement Bracket	0.04	0.02	3	Analysis
NICMOS Inlet Flex Lines	0.19	0.05	1	Test
Bayonet (Male and Female 6")	0.75	0.18	1	Test
Inlet Bayonet to Valve	0.03	0.03	3	Analysis
Inlet Cryovalve with heater	1.11	0.2	2	Test
Valve to Cryostat Shell	0.19	0.06	3	Analysis
Shell to Nitrogen Tank	0.02	0.01	3	Analysis
Nitrogen Tank to Shell	0.02	0.01	3	Analysis
Cryostat Shell to Valve	0.44	0.19	3	Analysis
Outlet Cryovalve with heater	1.11	0.2	2	Test
Valve to Outlet Bayonet	0.15	0.13	3	Analysis
Bayonet (Male and Female 3")	1.54	0.25	1	Test
NICMOS Outlet Flex Lines	0.26	0.05	1	Test
NICMOS Outlet Rigid Tubes	0.065	0.05	1	Test
Dewar	0.4	0.04	3	Analysis
Total from Test:	5.105	0.43	4	
Total from Analysis:	1.29	0.24	4	
Total:	6.395	0.49	4	

Notes:

1. Uncertainty is based on PRT limitations during test.
2. Uncertainty was reported from test engineer. Due to valve inconsistencies the parasitics range from 0.95 W to 1.11 W.
3. Uncertainty was reported from analyst.
4. Uncertainty was summed via adding in quadrature.

3.2 NCS system level thermal vacuum results

The NCS full-up thermal vacuum test consisted of the entire suite of flight hardware in final flight configuration, as shown in block diagram form in Figure 5. The test was designed to demonstrate specific performance requirements verifications of the NCS SM3B configuration through a series of instrument and thermal loads representative of on-orbit conditions, including HST predicted Hot and Cold and those predicted conditions plus 10ºC in addition to nominal[5]. The NCC Shunt was used as a surrogate NICMOS with the temperature of the NICMOS Dome derived indirectly by a weighted average of the Cold Load Interface (CLI) inlet and outlet temperatures providing a value for the ESM microprocessor.

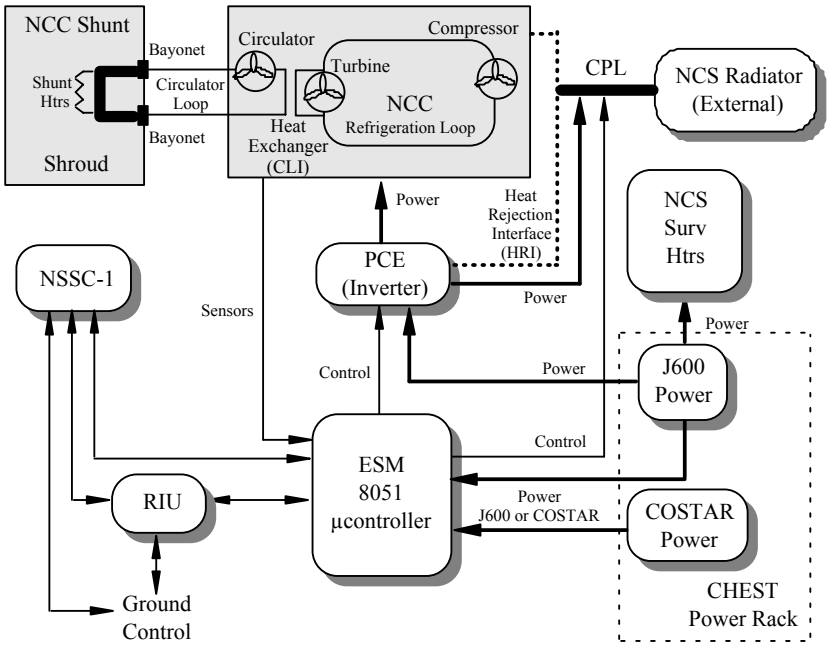

Figure 5 – NCS System Level Thermal Vacuum Test Block Diagram

All stability and repeatability measurements exceeded the top-level stability requirement of ±0.5K by maintaining the shunt within ±0.1K of the control set point over any one 1000 second period. Although the NCC Shunt does not mirror the dynamic thermal response of the NICMOS dewar, it responds much faster to environmental changes due to the much smaller thermal mass, the qualitative results indicated that the NCC control of NICMOS detector temperature was sufficiently demonstrated.

4. ON-ORBIT PERFORMANCE

The on-orbit performance of the NCS was validated during Servicing Mission Orbital Verification (SMOV) activities. SMOV consists of a pre-mission defined set of tests designed to exercise the newly installed hardware and its interaction with other HST hardware.

4.1 NCC performance

The NCC was started on the HST for the first time on March 17, 2002 (day 78), following on-orbit installation with a goal of reaching 70K at the NICMOS cooling coil. During the first 17days of the cooldown, the compressor was operated at a rate of 7100 revolutions per second (rps) to protect the true hardware compressor speed limit of 7300 rps. Due to internal NCC gas dynamics interaction between the compressor and turboalternator, the speed of the compressor "surges" above and below the commanded speed until the turboalternator inlet temperature falls below ~82K. Surging stopped 17 days into the cooldown and the commanded compressor speed was raised to 7300 rps. The NICMOS main electronic boxes (MEBs) were shut down on day 87 in order to minimize parasitics into the system and increase the cooldown rate, with the MEBs off temperature sensors in the dewar of NICMOS were unavailable and dewar cooldown was not monitored. On day 101 the setpoint of 70K was reached on the NCC average temperatures of the inlet and outlet gas and the NCC started regulating its compressor speed to keep the average temperature at 70K. A profile of the cooldown is provided in Figure 5.

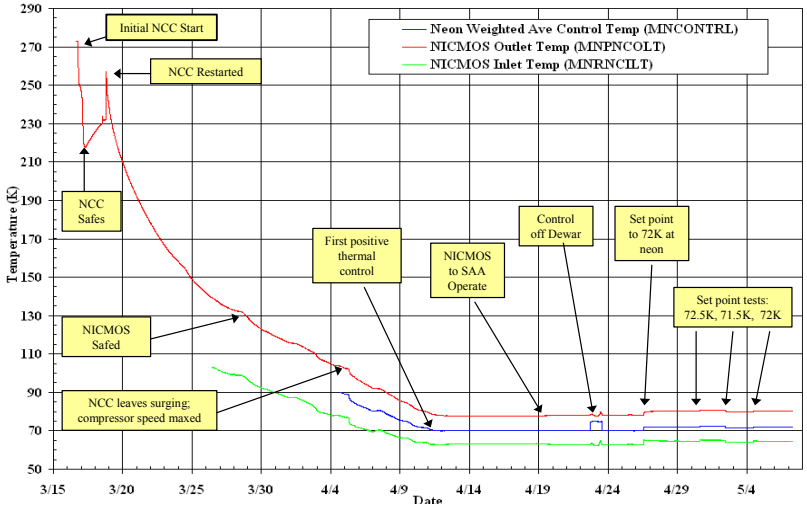

Figure 5 – NICMOS Cooldown Profile

At end of the cooldown the parasitic heat into the circulating loop of the NCC was calculated as 6.1 watts. On day 109 the NICMOS instrument was turned on and the heat parasitics into the system went to 6.5 watts. The average power used during the entire cooldown was 377 watts. The majority of this power went into running the NCC compressor and the remainder of the power went into running the Power Control Electronics, and the circulator.

A series of temperature set-point control tests were then performed to assess the stability/repeatibility of the control system and to determine the optimum set-point temperature for operation during the first year. With the NICMOS instrument enabled, the cooling coil temperature was systematically varied over a small temperature range (72K, then to 72.5K, then to 71.5K, and then back to 72K) with steady operation for periods of several days ranging up to a week at each temperature level. The results from these tests are shown in Figure 6, which plots the temperature on the NICMOS inlet and outlet tubes (MNRNCILT and MNRNCOLT), the computed control temperature (MNCONTRL) and a temperature measured at the NICMOS detector (NDWTMP11). Table 1 summarizes the important performance data at the selected set-point during the first six weeks of stable operation.

Table 1. NCC Performance Parameters Averaged from 5/10/02 to 6/18/02

Parameter	Average Value	Range
Detector temperature	77.10 K	77.03 K to 77.17 K
Cryostat cold dome temperature	72.41 K	72.39 K to 72.44 K
Gas temperature to NICMOS	65.04 K	64.95 K to 65.11 K
Gas temperature from NICMOS	80.54 K	80.47 K to 80.60 K
Heat rejection temperature	6°C	2°C to 10°C
Total cooling power	6.93 W	6.83 W to 7.02 W
Compressor rotational speed	7116 rev/s	7052 rev/s to 7208 rev/s
Compressor input power	315 W	307 W to 324 W

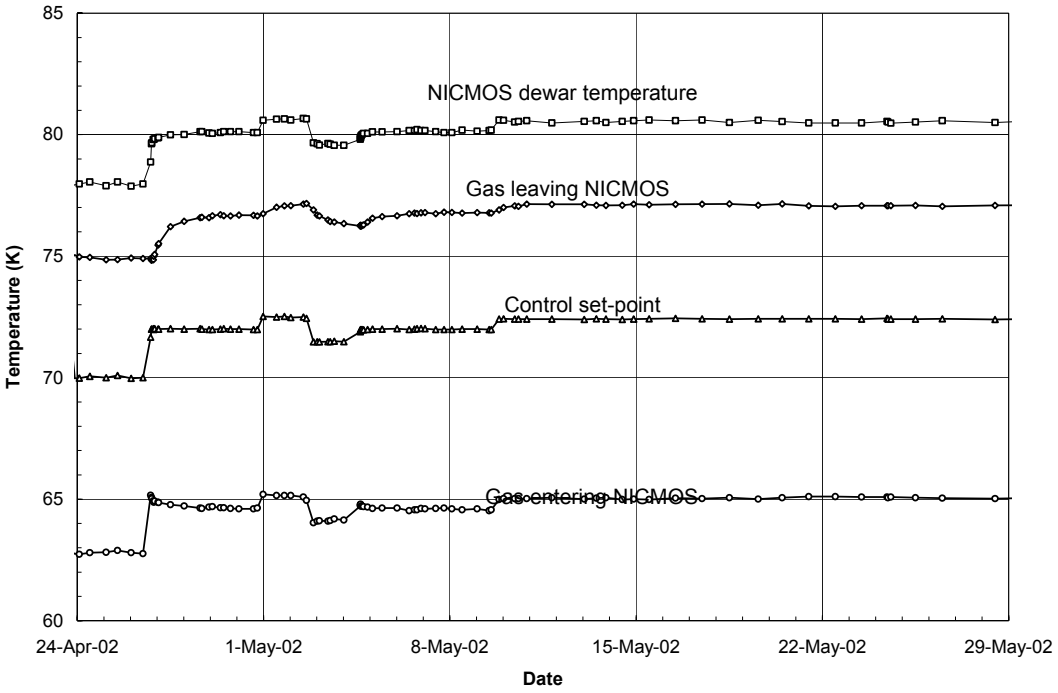

Figure 6 - Temperatures in the cryocooler and NICMOS during SMOV temperature control tests prior to setting the first-year operating conditions.

The NCC neon temperature can be controlled off of several control points. The control point that was used during cooldown was the average NCC inlet and outlet neon temperature. The other main control point was the NICMOS dewar sensor located close to the neon lines at the dewar. On day 112 a control test was done to determine if the neon temperature could be controlled off of the dewar. This test demonstrated that the dewar control was not feasible due to the thermal lag in the dewar. The dewar took approximately six hours to respond to a change in the neon temperature. This lag caused instability in the detector temperature and the control was put back onto the neon temperatures after 20 hours under dewar temperature control.

On day 129 a control setpoint of 72.4K was chosen to be the final operating setpoint on the average neon temperatures. Several things were taken into account when picking the final setpoint. First of all the scientists wanted to be able to monitor the detector temperature and the temperature sensor saturated at 77.43K . Second of all was that the final setpoint had to be maintained throughout all temperature extremes introduced by seasons and attitudes. The maximum predicted orbit average temperature of the radiator is –3°C which equates to +20°C at the compressor heat rejection plate.

4.2 CPL/Radiator performance

On day 94 (16 days into cooldown) it was decided that the minimum evaporator temperature that the CPL would be allowed to achieve would be –12°C. Before this point the minimum temperature allowed was -10°C. The change was made to help aid in the cooldown after on orbit data showed consistent and stable CPL and radiator operation. The NCC CPL setpoint ranged from –12C to +5C during cooldown (averaged about –8C).

The average radiator temperature during post-cooldown has been -18°C and the average CPL setpoint has been -8°C. The average compressor speed has been 7100rps. The detector has been holding steady at 77K.

4.3 NICMOS performance

The superb performance of the NCS hardware has resulted in the NICMOS instrument perfoming better than it had before. The ability to select an operating temperature for the detectors has allowed for optimizing detector performance (rather than optimizing the performance of the solid cryogen). The current operating temperature of the detectors is 77.1K, significantly warmer than the 62K operation with the solid cryogen. Almost all the scientific operating parameters for the instrument are the same as before, with only two parameters showing any difference. The dark current of the detectors is higher due to the higher operating temperature. This is still at a level that is low enough to allow the instrument to be background dominated for most observations. The warmer temperature also allows for a significant improvement in quantum efficiency. The current instrument is roughly 30 to 40% more sensitive for most observations. Table 2 summarizes the NICMOS scientific parameters for the current instrument.

Table 2. NICMOS Scientific Parameters

Parameter	Pre-NCS	Post-NCS	Units	Comments
Readout Noise	~30	~30	e^-/readout	no change
Dark Current	0.1	~0.15	e^-/pix/sec	
QE (F110W)	0.2	0.32		QE = quantum efficiency. F110W is short wavelength end (1.1 um) for NICMOS, F222M is long wavelength (2.2 um) end.
QE (F160W)	0.3	0.42		
QE (F222M)	0.6	0.72		
Focus				no change

5. FUTURE APPLICATIONS

Future NASA missions including the Terrestrial Planet Finder, Constellation-X, and the Next Generation Space Telescope will require the capability to reliably cool detectors and associated components to temperatures as low as 6 K with cooling loads from a few watts to several hundred milli-watts for extended periods.[4] The cooler technology developed for the NICMOS application can be extended to these future, more-demanding missions with current cooler technology development focused on smaller turbomachines and more compact recuperators compatible with the lower temperatures required for these missions.

6. ACKNOWLEGMENTS

Work on the NCS was performed for the NASA Goddard Space Flight Center under contracts NAS5-50000, NAS5-01090, and

7. REFERENCES

1. Dame, R.E., Cofie, E., Thomas, B.A.," A Post Launch Thermal Expansion Analysis of the Near Infrared and Multi-Object Spectrometer (NICMOS) Cryogenic Subsystem's Dewar", MEGA Engineering, Silver Spring, MD, 1997.
2. Cheng, E.S., Smith, R.C., Jedrich, N.M., Gibbon, J.A., Cottingham, D.A., Swift, W.L., Dame, R.E.; "The Near Infrared Camera and Multi-Object Spectrometer Cooling System"*; SPIE Proceedings 3356*, ed. P.Y. Bely, Kona, HI, 1998.
3. Jedrich, N.M., Zimbelman, D., Turczyn, M., Sills, J., Voorhees, C., Clapp, B.; "Cryo Cooler Induced Micro-Vibration Disturbances to the Hubble Space Telescope"; *5th Cranfield Space Dynamics Conference*, Cambridge, UK, 2002.
4. Jedrich, N.M., Zimbelman, D., Swift, W., Dolan, F.X.; "A Mechanical Cryogenic Cooler for the Hubble Space Telescope"; *39th Space Congress*, Cocoa Beach, FL, 2002.
5. Story, D.;"NICMOS Cooling System (NCS) SM3B Configuration System Level Thermal Vacuum Acceptance Report", Jackson & Tull, Seabrook, MD 2002.
6. Cottingham, C.E., Zagarola, M.V., Bugby, D.C., Russell, A. M.; "Testing Method to Determine the Thermal Parasitics of the NICMOS Cryogenic Cooler"; *31st International Congress on Environmental Systems*, Orlando FL, 2001